Asian Journal of Chemistry; Vol. 38, No. 3 (2026), 683-690
ASIAN JOURNAL OF CHEMISTRY
https://doi.org/10.14233/ajchem.2026.35006

Isolation and Characterisation of β-Sitosterol Derived from Indigenous Therapeutic Plant *Crateva religiosa* (Frost.) and its Anticancer Properties

SEBIN FERNANDEZ*, L. CATHRINE and F. VIRGINIA

PG and Research Department of Chemistry, Holy Cross College (Autonomous) (Affiliated to Bharathidasan University), Tiruchirappalli-620002, India

*Corresponding author: E-mail: sebinabraham2@gmail.com

Received: 4 October 2025 *Accepted*: 20 January 2026 *Published online*: 6 March 2026 AJC-22288

In this study, an indigenous medicinal plant, *Crateva religiosa*, was chosen to examine its anticancer potential with its pharmacological effects. This study aims to explore the anticancer potential of an underexplored medicinal plant source, coupled with detailed structural characterization and *in vitro* cytotoxicity evaluation. The FT-IR spectrum confirmed hydroxyl, alkene, and alkane functionalities, indicated by absorption peaks appearing at 3420, 1640 cm^{-1} and 2925-2850 cm^{-1}, respectively. ^{13}C NMR spectrum displayed 29 distinct carbon resonances, including characteristic olefinic carbons at δ 140.77 and 121.73 ppm. Mass spectrometric analysis further confirmed the molecular formula as $C_{29}H_{50}O$ with a prominent molecular ion peak at *m/z* 437.18, which was consistent with the expected mass of the isolated compound. The MTT-based *in vitro* cytotoxicity assay showed that β-sitosterol possesses anticancer effect against the A549 lung cancer and HeLa cervical cancer cell lines, with IC_{50} of 60.40 μg/mL and 57.11 μg/mL, respectively. Such findings indicate the remedial value of β-sitosterol extracted from *C. religiosa*, which proves to be a beneficial anticancer agent.

Keywords: *Crateva religiosa*, Anticancer activity, Phytochemical analysis, Cervical cancer.

INTRODUCTION

Cervical cancer is one of the most common cancers among women, posing a significant global health challenge [1,2]. This study addresses the issue through early detection and the development of affordable, plant-based drugs with minimal side effects [3,4]. Plant species are crucial for developing new treatments, particularly for drug-resistant cancers like cervical cancer, with many natural products such as alkaloids, flavonoids and terpenoids showing antitumor potential [5,6].

Certain plant compounds exhibit anticancer activity, influenced by the type of extract, treatment duration and plant species. *Crateva religiosa*, a flowering plant native to Asia and Africa, is recognized for its bioactive compounds, including essential oils and alkaloids. Traditionally, it has been used for various medicinal purposes, such as anthelmintic, diuretic and antioxidant [7-9]. In Ayurvedic medicine, Kanchnar Guggulu, derived from the bark of *C. religiosa*, has cytotoxic and antiproliferative properties [10]. Recent studies have highlighted the plant's anticancer potential against cervical, lung and breast cancers [9,10], but its specific effects on human cervical cancer (HeLa) cells remain untested.

The novel aspect of this work lies in identifying *C. religiosa* as a strong botanical source of anticancer phytosterols, particularly β-sitosterol, which exhibits well-documented pharmacological relevance [8,11]. Thus, characterizing β-sitosterol not only provides chemotaxonomic evidence but also enhances the credibility and reproducibility of the study. This dual approach offers insights into the pharmacological mechanisms of plant and establishes *C. religiosa* as a promising source of plant-derived anticancer agents. The research addresses a significant gap in understanding the cytotoxic effects of this plant on human cervical (HeLa) and lung cancer (A549) cells, paving the way for future therapeutic developments.

EXPERIMENTAL

Plant collection: The fresh plant specimen, comprising the leaves and stem of *Crateva religiosa*, was obtained from Ayurvedic Regional Research Institute, Thiruvananthapuram, India for the initial screening. The plant was authenticated by

scientists through documentation at the Jawaharlal Nehru Tropical Botanic Garden Research Institute, Thiruvananthapuram, India. The herbarium housed the plant under voucher specimen No: 98765.

Preparation of methanolic extract: Fresh plant material was thoroughly washed with tap water, chopped into small pieces and shade-dried for 15 days. The dried material was then grounded into a fine powder. A Soxhlet apparatus was used to extract 1000 g of this powder with 2000 mL of methanol. The resulting extract was filtered through Whatman No. 42 filter paper to remove insoluble residues and the filtrate was concentrated under reduced pressure using a rotary evaporator until a dry extract was obtained.

Biological evaluations

Cell lines and cell culture preparation: The A549 and HeLa cell lines were procured from the National Centre for Cell Science and cultured in Dulbecco's Modified Eagle's Medium (DMEM). This nutrient solution was supplemented with 10% fetal bovine serum, L-glutamine, Na_2CO_3 and antibiotics (penicillin, streptomycin, and amphotericin B) in 25 cm^2 tissue culture flasks. The cultures were maintained in an incubator at 37 ºC with 5% CO_2 and high humidity. To assess cellular viability, the MTT assay and inverted phase-contrast microscopy were employed. After 2 days of incubation, the cell monolayers were trypsinized and resuspended in growth medium supplemented with 10% serum for further analysis. A cell suspension of 5×10^3 cells per well was then added to tissue culture plates, which were incubated in a controlled humidified chamber at 37 ºC with 5% CO_2.

Cytotoxicity assay: The MTT compound was utilized in a colorimetric assay to evaluate the anticancer potential of freshly extracted methanolic leaf and stem samples from *C. religiosa*. A solution was prepared by dissolving 1 mg of MTT in 1 mL of 0.1% DMSO and processed in a cyclomixer. This solution was then filtered through a 0.22 μm Millipore syringe filter to ensure sterility. After preparing the extracts at concentrations of 100, 50, 25, 12.5, and 6.25 μg/mL, they were diluted in 500 μL of DMEM and added to triplicate wells. The plates were incubated for 24 h at 37 ºC with 5% CO_2, while control wells received no treatment under identical conditions. Post-incubation, an inverted phase-contrast microscope (Olympus CKX41 with Optika Pro5 CCD camera system) was employed to observe cell growth. Subsequently, 30 μL of MTT solution (15 mg in 3 mL PBS) was added to the wells and incubated for 4 h at 37 ºC [12]. After removing the supernatant, 100 μL of DMSO was added to dissolve the formazan crystals formed during the assay. The absorbance at 540 nm was determined by a reader on a microplate using the following formula:

$$\text{Cell viability (\%)} = \frac{OD_{test}}{OD_{control}} \times 100 \quad (1)$$

The IC_{50}, which is equivalent to a 50% decrease in cell count relative to the control, was also calculated.

Apoptosis studies using acridine orange (AO) and ethidium bromide (Etbr) double staining: A549 (human lung carcinoma) and HeLa (human cervical carcinoma) cells were cultured in 25 mL flasks using DMEM supplemented with L-glutamine, sodium bicarbonate (Merck), 10% fetal bovine serum (FBS), penicillin (100 U/mL), streptomycin (100 μg/mL), and amphotericin B (2.5 μg/mL). The cultures were maintained at 37 ºC in a humidified incubator with 5% CO_2 until confluency was reached after 24 h. The cells were then treated with the methanolic extract of leaves at the IC_{50} con-centration. Following treatment, the cells were washed with cold PBS and stained with acridine orange (AO, 100 μg/mL) and ethidium bromide (EtBr, 100 μg/mL) for 10 min. After rinsing, the stained cells were examined under a fluorescence microscope, where viable cells exhibited green fluorescence, while dead cells showed red fluorescence. Based on chromatin morphology and fluorescence characteristics, cells were classified as healthy (green nucleus), early apoptotic (bright green nucleus with condensed chromatin), late apoptotic (orange-stained nuclei) or necrotic (uniformly orange nuclei).

Enzyme-linked immunosorbent assay (Elisa): All the cells (A549 and HeLa) were cultured in 25 mL flasks separately containing DMEM supplemented with 10% fetal bovine serum, L-glutamine, sodium bicarbonate, penicillin (100 U/mL), streptomycin (100 μg/mL), amphotericin B (2.5 μg/mL) and maintained at 37 ºC in a humidified 5% CO_2 incubator. Cells were treated with the IC_{50} concentration of the methanolic leaf extract prepared from a 1 mg/mL stock solution [13] and incubated for 24 h. Culture supernatants were then collected and transferred to 96-well plates (100 μL per well) and incubated overnight at 37 ºC. After blocking with gelatin-Tween buffer for 1 h, the wells were incubated sequentially with primary antibody and HRP-conjugated secondary antibody (Santa Cruz, USA) [14], with PBS washing in between. The colour development was achieved using *o*-dianisidine hydrochloride substrate and the reaction was terminated by adding 5 N HCl. Finally, the absorbance was measured at 415 nm using an ELISA reader and the antibody activity was calculated using eqn. 2:

$$\text{Antibody activity} = \frac{\text{OD value}}{\text{Protein concentration}} \quad (2)$$

Fractionation of methanolic extract: Thin-layer chromatography (TLC) was employed to separate the constituents present in the crude methanolic extract of *C. religiosa* leaves and stems following preliminary fractionation by column chromatography. Approximately 21 g of dried methanolic extract was loaded onto a silica gel column. Elution was initiated with 100% hexane and the polarity of the mobile phase was gradually increased by the addition of chloroform and methanol. Separation of components occurred based on differences in polarity as the solvent system passed through the column [15] and fractions of 5 mL were collected. Fractions exhibiting similar R_f values were noted and selected for further structural characterization. The R_f value was determined using the following eqn.:

$$R_f = \frac{\text{Distance travelled solute}}{\text{Distance travelled by solvent}} \quad (3)$$

Characterisation: FT-IR analysis was performed to identify functional groups by recording spectra of KBr pellets in the range of 4000-400 cm^{-1}. NMR spectra were acquired on a Bruker AMX-500 spectrometer at 300 K, using tetra-

methylsilane or the residual solvent signal as the internal chemical shift reference, with coupling constants reported in hertz (Hz). Molecular weight determination and fragmentation analysis were carried out using high-resolution mass spectrometers including Thermo Finnigan MAT95XL, LTQ Orbitrap Velos, Agilent 6890 GC coupled with JMS-T100GC and a Thermo-Exactive system operated at a resolving power of 60,000.

Statistical analysis: All experiments were performed in triplicate and the results are presented as mean ± standard error. Statistical analysis was carried out using one-way ANOVA followed by Dunnett's post-hoc test, with ***p < 0.001 considered statistically significant compared to the control group [16].

RESULTS AND DISCUSSION

Herbal medicine, with its diverse phytochemical contents, has gained popularity in cancer treatment. Plant *C. religiosa*, identified at Odakkali Research Institute, contains several key phytochemicals such as phenols, tannins and flavonoids, which contribute to its medicinal values.

Isolation and structural characterization of β-sitosterol: β-Sitosterol was isolated from the methanolic extract using column chromatography with TLC-grade silica gel as the stationary phase. Elution was initiated with *n*-hexane, followed by a gradual increase in polarity through the controlled addition of ethyl acetate and finally methanol. Twenty fractions were collected (total volume 100 mL) and fraction 14 yielded β-sitosterol using an ethyl acetate:methanol solvent system. TLC analysis confirmed its identity, with fraction 14 showing a R_f value of 0.55 and a pale-yellow spot comparable to the standard β-sitosterol.

FTIR analysis: FT-IR and high-resolution mass spectrometric analyses further validated the isolated compound (Fig. 1). The FT-IR spectrum displayed characteristic alkane C–H stretching vibrations at 3000-2800 cm^{-1}, C=C stretching of an alkene at 1640-1600 cm^{-1}, O–H stretching indicative of a hydroxyl group at 1460-1380 cm^{-1} and CH_2 bending vibrations between 750-650 cm^{-1}, confirming the presence of a long aliphatic chain [17]. HR-MS analysis revealed a prominent molecular ion peak consistent with β-sitosterol ($C_{29}H_{50}O$), along with characteristic fragment ions typical of sterol compounds, thereby confirming its molecular formula and structure (Fig. 2) [18].

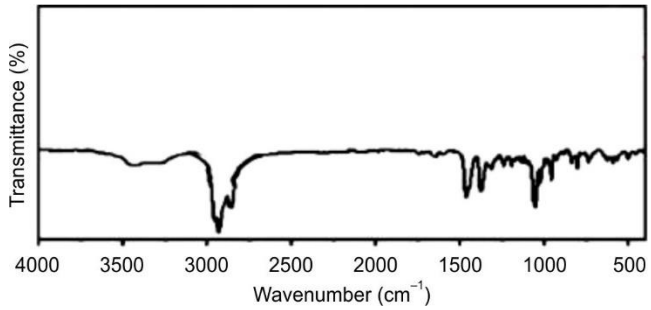

Fig. 1. FT-IR spectrum of β-sitosterol

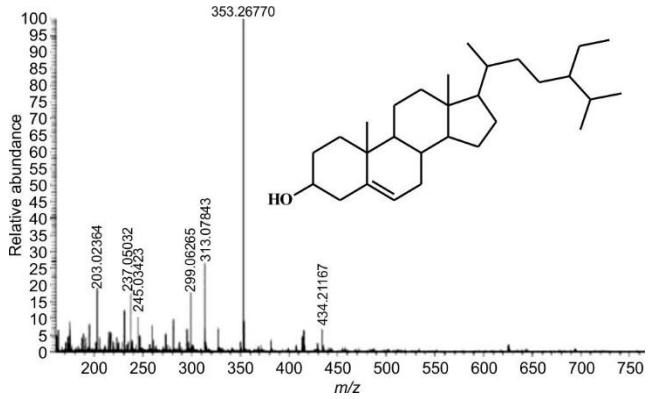

Fig. 2. HRMS of spectrum of β-sitosterol

NMR analysis: The structural confirmation was further obtained through comprehensive NMR analysis. The ^{1}H NMR spectrum (Fig. 3a) exhibited characteristic methyl proton signals between δ 0.65-1.05 ppm, a hydroxyl-bearing C3 proton at δ ~3.5 ppm and an olefinic proton at δ ~5.3 ppm corresponding to the Δ^5-sterol structure. The ^{13}C NMR spectrum (Fig. 3b) showed 29 distinct carbon signals, including aliphatic carbons (δ 11-40 ppm), a hydroxylated C3 carbon at δ ~71 ppm and olefinic carbons at δ ~140 and 121 ppm.

COSY correlations confirmed proton connectivity within the steroid backbone (Fig. 4a), while DEPT spectra clearly differentiated CH_3, CH_2 and CH groups, supporting the structural assignments (Fig. 4b). The absence of extraneous or oxidized functionalities and close agreement with reported spectral data confirm the purity and structural integrity of the isolated β-sitosterol [19].

Anticancer activity: The MTT assay of the methanolic leaves extract (Fig. 5a) quantitatively demonstrates a dose-

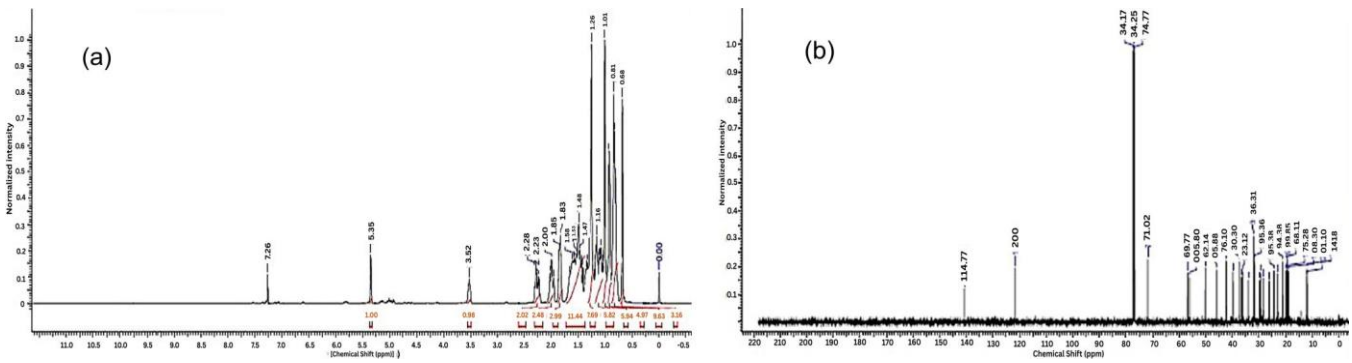

Fig. 3. (a) ^{1}H NMR and (b) ^{13}C NMR of β-sitosterol

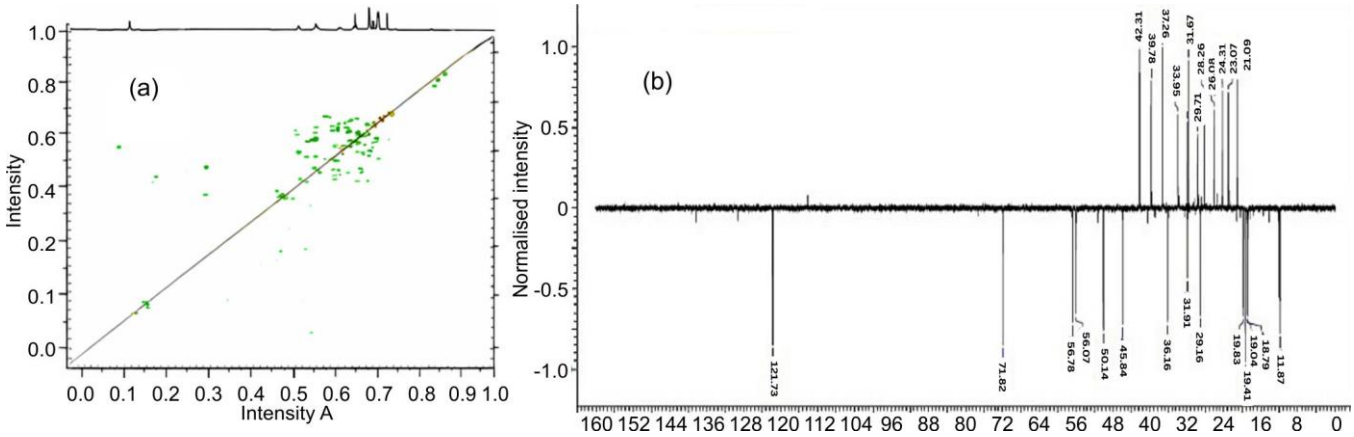

Fig. 4. (a) ^{1}H-^{1}H COSY spectrum and (b) DEPT spectrum of β-sitosterol

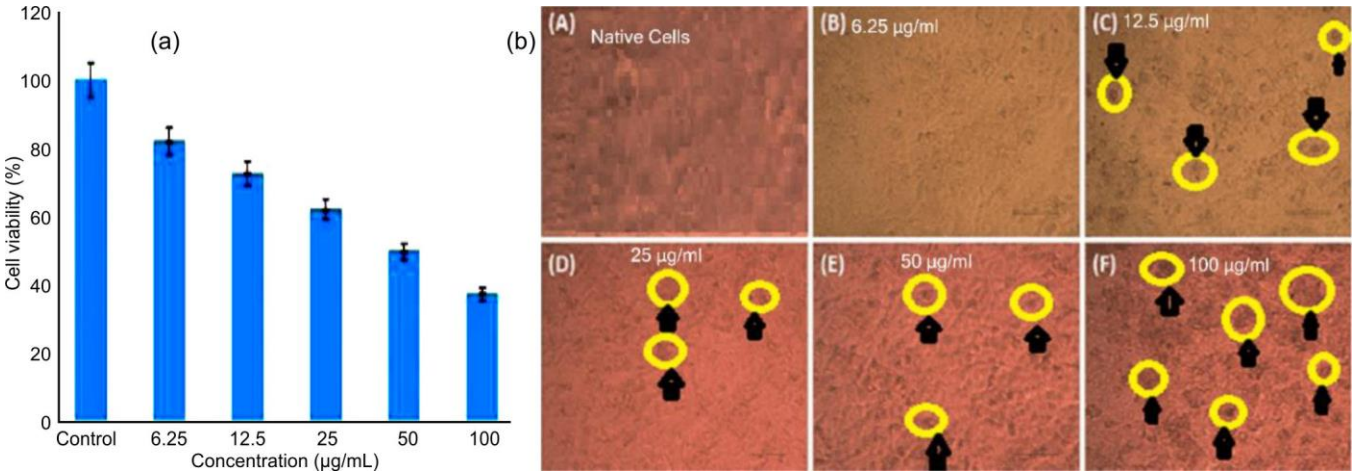

Fig. 5. (a) MTT assay data of methanolic extract leaves of *C. religiosa* and (b) morphological changes of the leaves extract on the control and treated lung cancer cell A549 lines

dependent decline in cell viability with increasing extract concentration, with the control group exhibiting complete viability as reflected by a mean optical density (OD) value of 0.7843. Treatment with 6.25 µg/mL of the methanolic extract resulted in a slight reduction in cell viability to 81.83 ± 0.17%, indicating low cytotoxicity. At 12.5 µg/mL, viability further decreased to 72.43 ± 0.11%, while markedly higher cell death was observed at 25 and 50 µg/mL, with viability values of 61.86 ± 0.07% and 49.59 ± 0.23%, respectively. A significant decline in viable cells was observed at the highest tested concentration of 100 µg/mL (37.09 ± 0.21%), suggesting strong antiproliferative activity. The bar graph illustrates a gradual and systematic decrease in cell viability with increasing extract concentration. The morphological analysis revealed normal cell shape and adherence in control cells, whereas treated cells exhibited progressive changes, including reduced adhesion at 6.25 µg/mL, membrane blebbing and cell shrinkage at 12.5 µg/mL, and pronounced rounding, membrane fragmentation and apoptotic body formation at 25 and 50 µg/mL. At 100 µg/mL and 256 µg/mL, extensive cytoplasmic shrinkage, complete cell detachment and membrane breakdown were observed (Fig. 5b), indicating dose-dependent cytotoxicity likely mediated through apoptotic and necrotic pathways in A549 cells.

The quantitative MTT assay of the methanolic extract of stem (Fig. 6a) revealed a clear concentration-dependent decline in cell viability. The control cells exhibited a high optical density (OD = 0.7843), corresponding to 100% viability. Upon exposure to 6.25 µg/mL, viability slightly decreased to 82.86 ± 0.01%, indicating mild cytotoxicity. Further reductions were observed at 12.5 µg/mL (77.84 ± 0.02%) and 25 µg/mL (58.27 ± 0.03%). Pronounced antiproliferative effects were recorded at 50 µg/ mL (42.87 ± 0.03%) and 100 µg/mL (35.09 ± 0.01%), confirming strong cytotoxic activity. These results are well illustrated in the accompanying bar graph, with narrow error margins indicating good experimental reproducibility.

Morphological analysis (Fig. 6b) supported the MTT findings, showing progressive structural damage with increasing extract concentration. Control cells retained normal morphology, appearing elongated, flattened and well adhered. Cells treated with 6.25 µg/mL showed mild alterations in adherence. At 12.5 µg/mL, early apoptotic features such as membrane blebbing and cell shrinkage were evident. More pronounced damage including cell rounding, detachment, membrane fragmentation, apoptotic bodies and cytoplasmic condensation, was observed at 25 and 50 µg/mL. At the highest concentration, severe morphological deterioration, membrane rupture and extensive cellular debris indicated the late-stage apoptosis or necrosis.

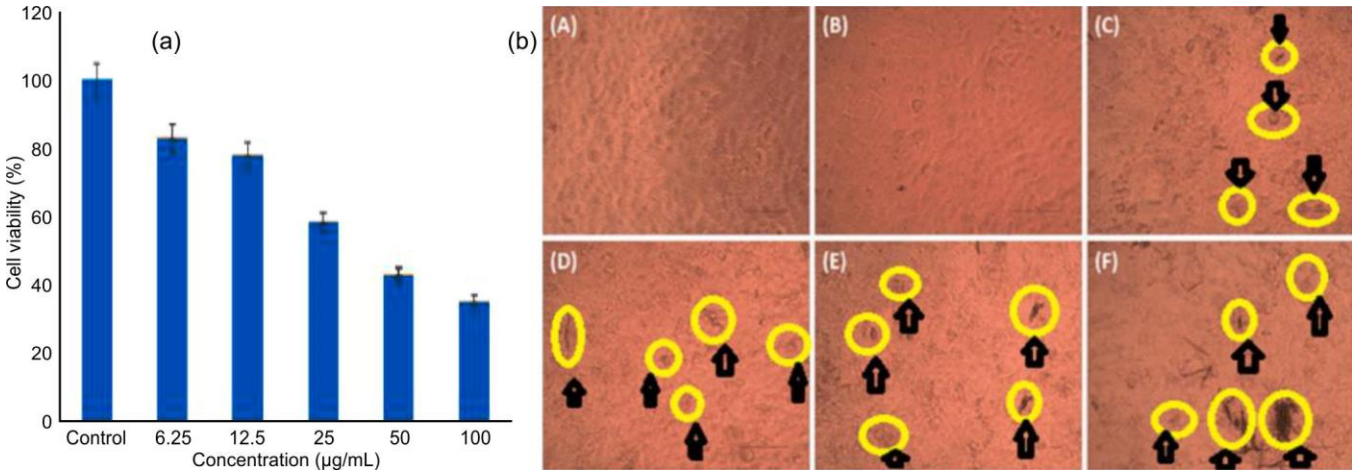

Fig. 6. (a) MTT assay data of methanolic extract of *C. religiosa* stem and (b) morphological changes of the stem extract on the control and treated lung cancer cell A549 lines

Based on the MTT assay data and morphological observations, Fig. 7 illustrates the cytotoxic effect of methanolic extract of *C. religiosa* leaves on HeLa cervical cancer cells. A dose-dependent decrease in cell viability was observed, with minimal cytotoxicity at 6.25 µg/mL (86.72 ± 0.002%). The viability further declined at 12.5 µg/mL (75.93 ± 0.02%) and 25 µg/mL (65.46 ± 0.01%). At higher concentrations of 50 and 100 µg/mL, cell viability decreased significantly to 51.24 ± 0.02% and 28.91 ± 0.01%, respectively, indicating strong antiproliferative activity (Fig. 7a). The bar graph highlights this concentration-dependent trend with low standard deviations, confirming reproducibility.

Microscopic examination further validated these findings, revealing concentration-dependent morphological changes in the HeLa cells. Untreated control cells exhibited typical epithelial morphology with tightly packed, flattened and polygonal features. Mild structural changes were observed at 6.25 µg/mL, while pronounced apoptotic features such as membrane blebbing, cell contraction and apoptotic body formation appeared at 12.5 µg/mL. At 25 and 50 µg/mL, extensive rounding, membrane fragmentation and loss of adhesion indicated progression toward advanced apoptosis. Treatment at 100 µg/mL caused severe cytoplasmic condensation, widespread detachment and disruption of monolayer integrity, consistent with late apoptosis or secondary necrosis (Fig. 7b).

HeLa cervical cancer cells were further subjected to a concentration-dependent MTT assay using the methanolic extract of stem (Fig. 8a). Cell viability decreased from 88.87 ± 1.20% at 6.25 µg/mL to 31.33 ± 2.08% at 100 µg/mL, confirming dose-dependent cytotoxicity. Similarly, the optical density values declined from 0.7025 in the control to 0.2201 ± 0.02 at the highest concentration. The microscopic images (Fig. 8b) showed intact cellular architecture in control cells, whereas treated cells exhibited progressive shrinkage, membrane blebbing and loss of integrity. The IC_{50} value of the stem extract against HeLa cells was determined to be 61.33 µg/mL.

Apoptotic activity: Apoptotic activity was further assessed through caspase-3 activation studies. As a key executioner enzyme in apoptosis, caspase-3 activity increased significantly following extract treatment, while cell numbers declined. Normalization of enzymatic activity to cell count ensured reliable assessment. AO/EtBr staining (Fig. 9a) demonstrated the presence of live, early apoptotic, late apoptotic and necrotic cells, with IC_{50} treated cells predominantly exhibiting late

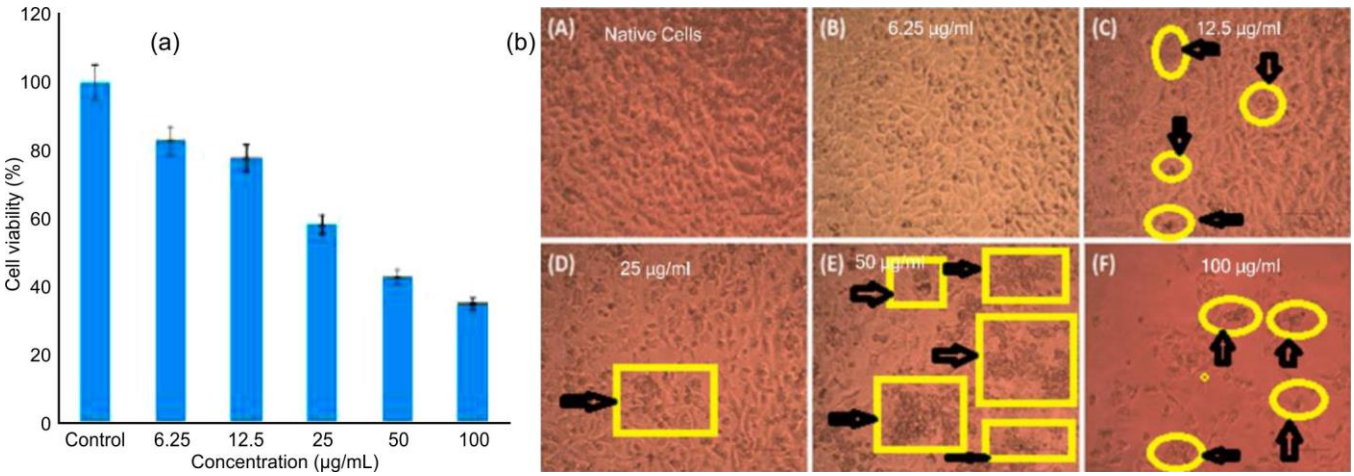

Fig. 7. (a) MTT assay of methanolic extract of *C. religiosa* leaves on HeLa cell lines and (b) photomicrographs of the anticancer effect of *C. religiosa* leaves extract on developed HeLa cells

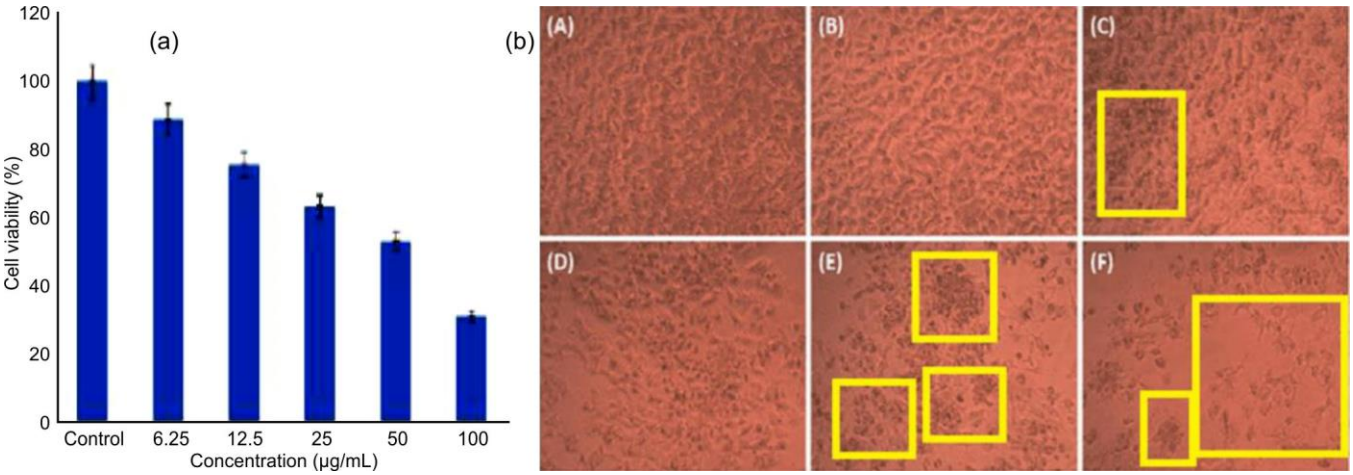

Fig. 8. (a) MTT assay of methanolic extract of *C. religiosa* stem on HeLa cell lines and (b) photomicrographs of the anticancer effect of methanolic extract of *C. religiosa* stem on developed HeLa cells

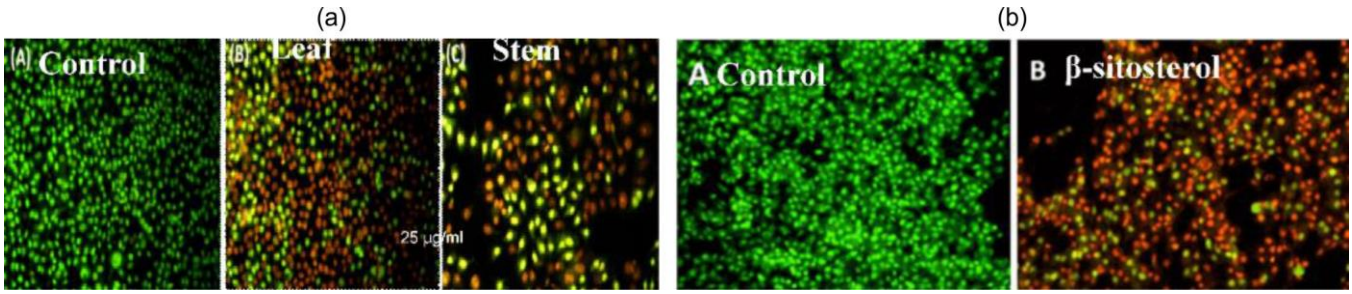

Fig. 9. Photomicrographs of apoptotic effect of *C. religiosa* extract on cultured HeLa cells (a) control and methanolic extract of leaf and stem and (b) control and β-sitosterol

apoptotic characteristics. β-Sitosterol-treated HeLa cells (Fig. 9b) similarly showed increased late apoptotic features, characterized by orange-stained nuclei and condensed chromatin.

Cytotoxic evaluation: Cytotoxic evaluation of isolated β-sitosterol demonstrated strong anticancer activity against HeLa cells. Untreated cells displayed healthy morphology, whereas treated cells exhibited progressive apoptotic changes with increasing concentration. Cell viability decreased from 79.39 ± 0.02% at 6.25 µg/mL to 40.91 ± 0.03% at 100 µg/mL, confirming dose-dependent cytotoxicity (Fig. 10).

The comparative analysis (Table-1) revealed that β-sitosterol isolated from *C. religiosa* exhibited a low IC_{50} value (57.11 µg/ mL), comparable to melittin and superior to other plant derived β-sitosterol sources, highlighting its therapeutic potential.

Indirect ELISA test to detect Caspase 3: The IC_{50} values of the methanolic leaves (58.88 µg/mL) and stem (61.33 µg/mL) extracts were evaluated using a 1 mg/mL stock solution. Cells were incubated at 37 ºC for 24 h in a humidified 5% CO_2 atmosphere, while control cells remained untreated.

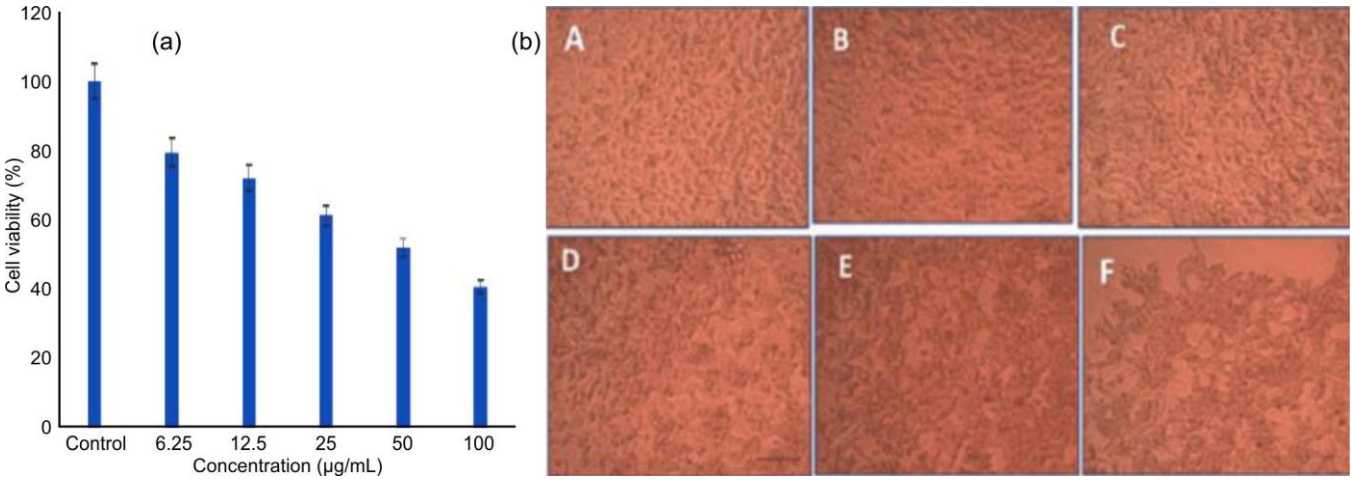

Fig. 10. (a) Graphical illustration of anticancer activity of β-sitosterol and (b) photomicrographs of anticancer impact of β-sitosterol on HeLa cells; (A) raw control cells, (B) 6.25, (C) 12.5, (D) 25, (E) 50 and (F) 100 µg/mL

TABLE-1
ANTICANCER IC_{50} VALUES OF PLANT-BASED AGENTS (AGAINST HeLa CELLS)

Plant source	Compound/extract	Cell line	IC_{50} (µg/mL)	Ref.
Crateva religiose	β-Sitosterol	HeLa	57.11	Present study
Catharanthus roseus	Gold nanoparticles	HeLa	65.3	[20]
Ganoderma applanatum	Crude extract	HeLa	68.4	[21]
Malva parviflora	β-Sitosterol	HeLa	70.2	[22]
Premna herbacea	β-Sitosterol	HeLa	73.5	[23]
Formononetin (herbal)	Isoflavone compound	HeLa	62.3	[24]
Melittin (bee venom)	Peptide extract	HeLa	56.7	[25]
Hohenbuehelia serotine	Polyphenol extract	HeLa	59.5	[26]
Baccaurea macrocarpa	β-Sitosterol & stigmasterol	HeLa	71.2	[27]
Crateva nurvala	Methanolic bark extract	HeLa	75.6	[28]

TABLE-2
INDIRECT ELISA TEST TO DETECT CASPASE-3 HeLa (HUMAN CERVICAL CANCER) CELLS

Samples	Absorbance at 415 nm	Protein concentration	Activity units/mg protein
Control	0.2748 ± 0.01	3.6840 ± 0.13	0.0746 ± 0.001
Methanolic stem extract	0.3814 ± 0.04	2.7281 ± 0.11	0.1398 ± 0.001
Methanolic leaf extract	0.4783 ± 0.01	2.6240 ± 0.14	0.1823 ± 0.001

Antioxidant enzyme activity was assessed through absorbance at 415 nm, protein concentration and specific activity (units/mg protein). The control sample exhibited an absorbance of 0.2748 ± 0.01, protein content of 3.6840 ± 0.13 mg/mL and enzyme activity of 0.0746 ± 0.001 units/mg protein. The methanolic stem extract showed increased absorbance (0.3814 ± 0.04) with reduced protein content (2.7281 ± 0.11 mg/mL), resulting in higher enzyme activity (0.1398 ± 0.001 units/mg protein). Notably, the methanolic leaf extract displayed the highest absorbance (0.4783 ± 0.01), lowest protein concentration (2.6240 ± 0.14 mg/mL) and maximum specific activity (0.1823 ± 0.001 units/mg protein), indicating superior antioxidant potential (Table-2).

The enhanced enzymatic activity observed for both extracts supports their role in inducing oxidative stress mediated anticancer effects. β-Sitosterol is proposed to exert its anticancer activity through membrane disruption and boost of intracellular reactive oxygen species, leading to mitochondrial dysfunction and subsequent activation of caspase-3, as confirmed by ELISA analysis. The resulting nuclear fragmentation and chromatin condensation observed through AO/EtBr staining are consistent with apoptosis induction and align well with previously reported mechanisms of β-sitosterol mediated cell death.

Conclusion

This study establishes *Crateva religiosa* as a promising botanical source of potent anticancer agents, particularly β-sitosterol. The methanolic extracts of leaves and stem demonstrated significant cytotoxic activity against HeLa cervical cancer and A549 lung cancer cell lines, with IC_{50} values of 58.88 µg/mL and 60.40 µg/mL (leaves) and 61.33 µg/mL and 59.38 µg/mL (stem), respectively. Furthermore, the isolated β-sitosterol exhibited the highest efficacy with an IC_{50} of 57.11 µg/mL against HeLa cells. The mechanism of action was confirmed through apoptotic assays and ELISA analysis, showing that β-sitosterol induced apoptosis *via* caspase-3 activation, ROS generation and mitochondrial disruption. The AO/EtBr staining revealed characteristic morphological changes associated with early and late-stage apoptosis. The compared with similar plant-based anticancer agents reported in the literature, *C. religiosa* demonstrated superior or comparable efficacy. These findings suggest its potential as a lead candidate for developing plant-derived chemotherapeutic agents. However, further *in vivo* studies and clinical validation are necessary to establish safety, bioavailability and therapeutic efficacy in a biological system. This work contributes a novel insight into the pharmacological potential of *C. religiosa* and supports its future development for cervical and lung cancer therapies.

ACKNOWLEDGEMENTS

The authors gratefully acknowledge Mrs. Usha, Jawaharlal Nehru Tropical Botanic Garden and Research Institute, Palode, Thiruvananthapuram, for her assistance with plant identification.

CONFLICT OF INTEREST

The authors declare that there is no conflict of interests regarding the publication of this article.

DECLARATION OF AI-ASSISTED TECHNOLOGIES

During the preparation of this manuscript, the authors used an AI-assisted tool(s) to improve the language. The authors reviewed and edited the content and take full responsibility for the published work.

REFERENCES

1. Y. Li, K. Zheng, Q. Xu, L. Xie and H. Lu, *BMC Public Health*, **25**, 4271 (2025); https://doi.org/10.1186/s12889-025-25029-5
2. Y. Son, S. Hong, W. Jang, S. Kim, H. Lee, S. Lee, J. Kang, L. Smith and D.K. Yon, *Int. J. Gynecol. Cancer*, **36**, 102751 (2026); https://doi.org/10.1016/j.ijgc.2025.102751

3. S.L. Bedell, L.S. Goldstein, A.R. Goldstein and A.T. Goldstein, *Sex. Med. Rev.*, **8**, 28 (2020); https://doi.org/10.1016/j.sxmr.2019.09.005
4. G. Moriasi, M. Ngugi, P. Mwitari and G. Omwenga, *BMC Complement. Med. Ther.*, **25**, 379 (2025); https://doi.org/10.1186/s12906-025-04923-w
5. M. He, L. Xia and J. Li, *Biomolecules*, **11**, 1539 (2021); https://doi.org/10.3390/biom11101539
6. Z. Yao, Q. Wu, W. Sheng, X. Zhou, L. Cheng, X. Tian, H. Yuan, L. Gong, W. Wang, B. Li and C. Peng, *Fitoterapia*, **177**, 106099 (2024); https://doi.org/10.1016/j.fitote.2024.106099
7. R. Mohanapriya, T.V.R. Kumar and K.N. Sunil Kumar, *J. Res. Siddha Med.*, **4**, 67 (2021); https://doi.org/10.4103/jrsm.jrsm_12_22
8. P. Meenaloshini, A. Thirumurugan, S. Achiraman and T.S. Kumar, *J. Ethnopharmacol*., **353 (Part A)**, 120354 (2025); https://doi.org/10.1016/j.jep.2025.120354
9. M.S. Hossain, M.A.M. Patwary, S.A. Rupa, M. Kazi, A. Kumar, K.M. Alghamdi, M.M. Matin and M.R. Rahman, *J. Cancer*, **16**, 2492 (2025); https://doi.org/10.7150/jca.94492
10. P. Tomar, Y.N. Dey, D. Sharma, M.M. Wanjari, S. Gaidhani and A. Jadhav, *J. Integr. Med.*, **16**, 411 (2018); https://doi.org/10.1016/j.joim.2018.10.001
11. M. Parveen, A. Aslam, S. Siddiqui, M. Tabish and M. Alam, *J. Mol. Struct*., **1251**, 131976 (2022); https://doi.org/10.1016/j.molstruc.2021.131976
12. S. Soltanian, M. Sheikhbahaei and N. Mohamadi, *J. Appl. Pharm. Sci*., **7**, 142 (2017); https://doi.org/10.7324/JAPS.2017.70722
13. S. Aydin, E. Emre, K. Ugur, M.A. Aydin, I. Sahin, V. Cinar and T. Akbulut, *J. Int. Med. Res.*, **53**, 03000605251315913 (2025); https://doi.org/10.1177/03000605251315913
14. R. Hidayat and P. Wulandari, *Bioscientia Medicina: J. Biomed. Transl. Res.*, **5**, 447 (2021); https://doi.org/10.32539/bsm.v5i5.228
15. O. Coskun, *North. Clin. Istanb.*, **3**, 156 (2016); https://doi.org/10.14744/nci.2016.32757
16. Z. Ali and S.B. Bhaskar, *Indian J. Anaesth.*, **60**, 662 (2016); https://doi.org/10.4103/0019-5049.190623
17. A.H. Bhat, A. Alia, G.M. Rather and B. Kumar, *Int. J. Scientific Res. Biol. Sci.*, **6**, 111 (2019); https://doi.org/10.26438/ijsrbs/v6i2.111118
18. G. Gachumi and A. El-Aneed, *J. Agric. Food Chem.*, **65**, 10141 (2017); https://doi.org/10.1021/acs.jafc.7b03785
19. V. Yamin Jirjees and A. Ali Salih Al-Hamdani, *Bull. Chem. Soc. Ethiop.*, **39**, 1317 (2025); https://doi.org/10.4314/bcse.v39i7.7
20. V. Mani, K.S. Gopinath, N. Varadharaju, D. Wankhar and A. Annavi, *Nano TransMed.*, **3**, 100049 (2024); https://doi.org/10.1016/j.ntm.2024.100049
21. S. Chandra, M. Gahlot, A.N. Choudhary, S. Palai, R.S. de Almeida, J.E.L. de Vasconcelos, F.A.V. dos Santos, H.D.M. de Farias and H.D.M. Coutinho, *Food Chem. Adv.*, **2**, 100239 (2023); https://doi.org/10.1016/j.focha.2023.100239
22. M.S. Al Hasan, M.S. Bhuia, R. Chowdhury, M. Shadin, E. Mia, N.T. Yana, I.H. Rakib, S.A. Ansari, I.A. Ansari, H.D.M. Coutinho and M.T. Islam, *S. Afr. J. Bot.*, **180**, 431 (2025); https://doi.org/10.1016/j.sajb.2025.03.004
23. B.C. Lalremruata, P.C. Vanlalhluna, G. Singh and C. Tagitinin, *S. Afr. J. Bot.*, **177**, 472 (2025); https://doi.org/10.1016/j.sajb.2024.12.012
24. S. Elayaperumal, Y. Sivamani, P. Agarwal and N. Srivastava, *Nano TransMed.*, **4**, 100086 (2025); https://doi.org/10.1016/j.ntm.2025.100086
25. A. Rangayasami, K. Kannan and M. Subban, *Macromol. Symp.*, **400**, 2100085 (2021); https://doi.org/10.1002/masy.202100085
26. D.S. Bharathi, A. Boopathyraja, S. Nachimuthu and K. Kannan, *J. Cluster Sci.*, **33**, 2499 (2022); https://doi.org/10.1007/s10876-021-02170-w
27. A. Lakshmanan, P. Surendran, S.S. Priya, K. Balakrishnan, P. Geetha, P. Rameshkumar, T.A. Hegde, G. Vinitha and K. Kannan, *J. Photochem. Photobiol. Chem.*, **402**, 112794 (2020); https://doi.org/10.1016/j.jphotochem.2020.112794
28. K. Karthik, S. Dhanuskodi, C. Gobinath, S. Prabukumar and S. Sivaramakrishnan, *J. Phys. Chem. Solids*, **112**, 106 (2018); https://doi.org/10.1016/j.jpcs.2017.09.016